Characterization of the microstructure of dairy systems using automated image analysis

Juliana V.C. Silva, David Legland, Chantal Cauty, Irina Kolotuev, Juliane Floury

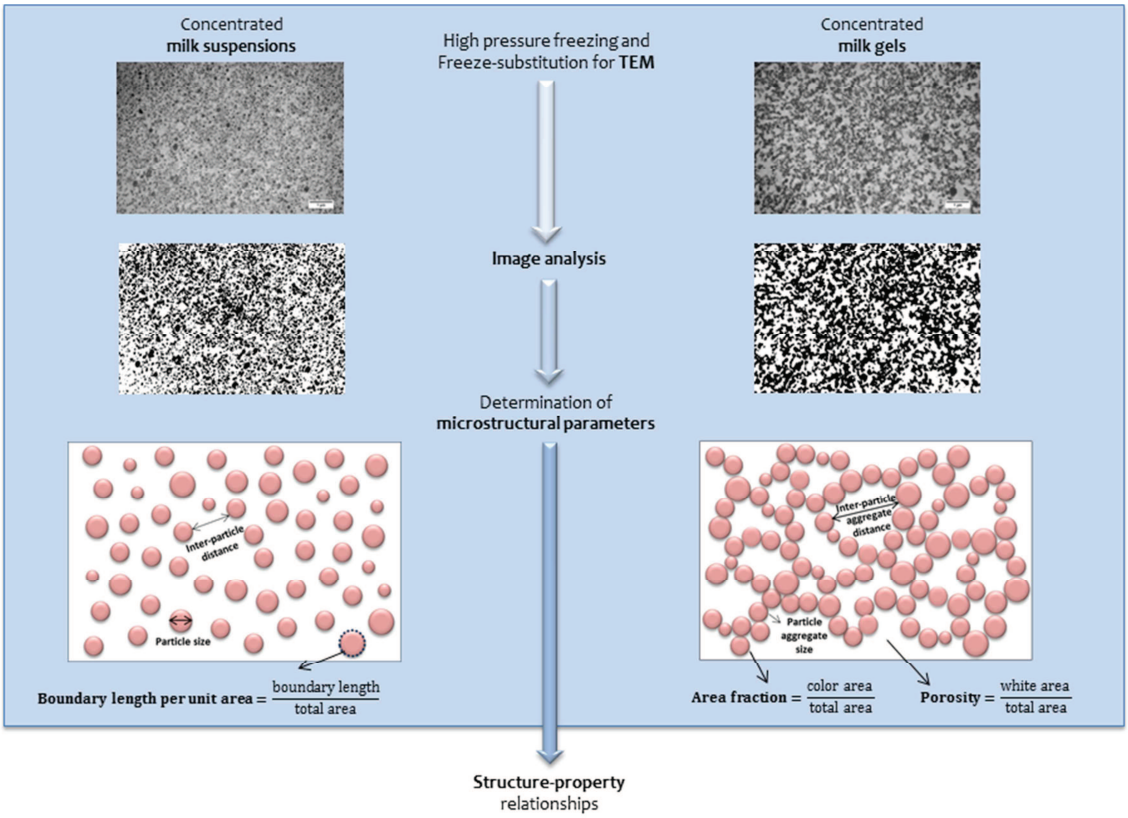

Characterization of the microstructure of dairy systems using automated image analysis

Juliana V. C. Silva[a], David Legland[b,c,d,e], Chantal Cauty[a], Irina Kolotuev[f,g], Juliane Floury[a,h,*]

[a]INRA, UMR1253 Science and Technology of Milk and Eggs, F-35042 Rennes, France

[b]INRA, UMR782 Food Process Engineering and Microbiology, F-78850 Thiverval-Grignon, France

[c]AgroParisTech, UMR782 Food Process Engineering and Microbiology, F-78850 Thiverval-Grignon, France

[d]INRA, UMR1318 Institut Jean-Pierre Bourgin, F-78026 Versailles, France

[e]AgroParisTech, Institut Jean-Pierre Bourgin, F-78026 Versailles, France

[f]MRic-TEM, UMS3480 Microscopy Rennes Imaging Center, F-35043 Rennes, France

[g]IGDR, UMR6290 University of Rennes 1, 2, F-35043 Rennes, France

[h]Agrocampus Ouest, UMR1253 Science and Technology of Milk and Eggs, F-35042 Rennes, France

[1]Corresponding author: Juliane Floury

Telephone number: +33 (0)2 23 48 54 52; Fax number: +33 (0)2 23 48 55 78

E-mail: juliane.floury@agrocampus-ouest.fr

ABSTRACT

A sound understanding of the microstructure of dairy products is of great importance in order to predict and control their properties and final quality. The aim of this study was to develop an automated image analysis procedure to characterize the microstructure of different dairy systems. A high pressure freezing coupled with freeze-substitution (HPF-FS) protocol was applied prior to transmission electron microscopy (TEM) in order to minimize any modification of the microstructure of the dairy systems investigated. The developed image analysis procedure was first validated on synthetic images of suspensions, and then on two types of concentrated milk suspensions. Microstructural data relating to casein micelles in milk suspensions were taken from the literature. The established procedure was then applied to the two corresponding rennet-induced milk gels, prepared from the same milk concentrates used for suspensions preparation. The automated image analysis procedure allowed the reliable estimation of several characteristic microstructural parameters including area fraction, porosity, boundary length per unit area, particle aggregate size, inter-particle aggregate distance and tortuosity. The relative ease of estimating these microstructural parameters from the automated image analysis method could make it useful for routine measurements of milk gels. Moreover, the method enabled a useful discrimination between two different types of milk gels. This novel approach can contribute to a better understanding of the effects of processing on the structure-property relationships in dairy products, and may be applied to other food systems.

Keywords: Transmission electron microscopy, microstructure, dairy systems, milk gels, freeze-substitution, quantitative image analysis

1. Introduction

The microstructure is one of the major determining factors of flavor, physicochemical and of the functional properties of dairy products. Thus understanding the microstructure of dairy products during their manufacture and subsequent storage is of great importance in order to predict and control their properties and final quality (Gunasekaran & Ding, 1999; El-Bakry & Sheehan, 2014).

Dairy products are principally based on caseins, which make up 80% of the protein in milk. Around 95% of the caseins in milk exist as large colloidal particles between 50 and 600 nm in diameter (mean ~120 nm), which are known as "casein micelles" (Fox & Brodkorb, 2008). The microstructure of dairy products depends principally on the organization of these casein micelles that can change as a function of the technological treatment applied to milk. For instance, casein micelles are easily destabilized by adding rennet to milk to form a rennet-induced gel, the basis of cheese making (Lucey, 2002; Dalgleish & Corredig, 2012). In contrast to milk, where caseins are present in suspension, milk gels form a continuous three dimensional network whose properties greatly depend on the microstructure.

The microstructure of dairy products is commonly investigated using instrumental techniques such as light or electron microscopy techniques. Light microscopy, such as Confocal Laser Scanning Microscopy (CLSM), allows the observation of dairy products with a minimum of sample preparation and with a resolution up to 0.25 microns (Fenoul, Le Denmat, Hamdi, Cuvelier, & Michon, 2008; Morand, Guyomarc'h, Legland, & Famelart, 2012; Ercili-Cura et al., 2013). By using this technique, it may be possible to distinguish the structure of the milk gel, but not the fine organisation of casein micelles that form its microstructure. Electron microscopy provides a resolution at a nanometer scale, making it possible to observe the organization of the gel protein network itself. Scanning Electron

Microscopy (SEM) has already been used for investigating the microstructure of a variety of dairy products (Marchesseau, Gastaldi, Lagaude, & Cuq, 1997; McMahon, Fife, & Oberg, 1999; Fallico et al., 2006; Le Feunteun & Mariette, 2007; 2008). However, SEM provides only a topographical view of the sample surface, making it difficult to quantify properties from the observed images. On the other hand, Transmission Electron Microscopy (TEM) provides observation of a slice of the sample, making it possible to investigate its internal structure. This can provide a basis for the quantitative description of the sample microstructure (Reis & Malcata, 2011).

Conventional TEM preparation procedures include chemical fixation, dehydration and embedding, which are frequently problematic in samples with high water content. Such methods can introduce numerous artifacts that alter the relationships that exist between the structural components (Kalab, Allan-Wojtas, & Mistry, 1995). Therefore, the use of low-temperature methods, such as freeze-fracture replication (Büchheim, 1982; McMahon & McManus, 1998), freeze-substitution (Goff, Verespej, & Smith, 1999; Smith, Kakuda, & Goff, 2000), cryo-TEM (Waninge, Nylander, Paulsson, & Bergenstahl, 2003; 2004) and high pressure freezing coupled with freeze-substitution methods (Ramasubramanian, Webb, D'Arcy, & Deeth, 2013) are preferable in order to preserve the original structure of the dairy sample ahead of the conventional TEM.

Nowadays, qualitative interpretations of micrographs are often no longer enough. Image analysis is necessary to also provide quantitative data for the analysis and design of food microstructure (Aguilera, Stanley, & Baker, 2000). Such image analysis has been recently introduced into dairy research for a wide range of applications (Wium, Pedersen, & Qvist, 2003; Impoco, Carrato, Caccamo, & Tuminello, 2006; Rovira, Lopez, Ferrandini, & Laencina, 2011; Geng, van den Berg, Bager, & Ipsen, 2011; Ong, Dagastine, Kentish, & Gras, 2011; 2012; 2013).

Micrograph images of dairy samples can be quantified through the morphometry of individual objects or particles (Gunasekaran & Ding, 1999; Rovira et al., 2011; Impoco, Fucà, Pasta, Caccamo, & Licitra, 2012; Fucà, Pasta, Impoco, Caccamo, & Licitra, 2013). When a protein network cannot be easily segmented, gray level texture analysis can be used to discern the variations of gray levels from confocal images (Fenoul et al., 2008; Morand et al., 2012; Ercili-Cura et al., 2013). An alternative to particle-based image analysis and image texture analysis is the characterization of protein network as a binary microstructure. This method consists of quantifying geometrical properties of a structure that cannot be described by a set of individual particles, but rather as a complex structure with voids and branches that is observed in a representative window. While this approach is common in materials science (Ohser & Mücklich, 2000) and for describing porous media (Torquato, 2002), to the authors' knowledge no attempt have been made to quantify the microstructure of dairy products.

The aim of this work was thus to develop an automated image analysis procedure to characterize the microstructure of dairy systems. The proposed procedure comprised the automated segmentation of the protein network from TEM micrographs, and the subsequent computation of microstructural parameters by assimilating the protein network to a porous media. The high pressure freezing and freeze-substitution (HPF-FS) protocol was used in order to minimize modification of the microstructure of dairy systems during sample preparation for TEM. Microstructural parameters considered in this study included global morphological parameters (area fraction, porosity, boundary length per unit area), binary image granulometry, that measures the typical sizes of particles (or of particle aggregates or of voids), and a tortuosity parameter that describes the microstructure at a larger scale. Tortuosity is a parameter mainly related to mass transfer properties and has been measured in several porous media such as rocks, sediments, soil, zeolites, biological tissues, etc. (Suman & Ruth, 1993; Latour, Kleinberg, Mitra, & Sotak, 1995; Zalc, Reyes, & Iglesia, 2004; Wu, van

Vliet, Frijlink, & van der Voort Maarschalk, 2006; Shen & Chen, 2007; Lanfrey, Kuzeljevic, & Dudukovic, 2010). Some authors have also been applying the theory of porous media to food systems and have been estimating tortuosity values from diffusion coefficients in food media (Crossley & Aguilera, 2001; Sam Saguy, Marabi, & Wallach, 2005). The determination of tortuosity directly from image analysis would therefore be of great interest for understanding the diffusion phenomena in dairy products.

The concept of measuring the above listed parameters using image analysis was first tested on a synthetic image representing a suspension of micelles as might be observed under conditions similar to the present study. The image analysis method was subsequently validated on two concentrated milk suspensions of similar casein concentration, but produced by different methods. Microstructural data relating to casein micelles in milk suspensions were taken from the literature for validation. The method was then applied to the corresponding concentrated milk gels, obtained by rennet-induced coagulation of the same milk concentrates used for suspensions preparation, in order to show a wider application of this procedure.

2. Material and Methods

2.1. Preparation of concentrated milk suspensions and gels

Two concentrated milk suspensions and two concentrated milk gels presenting similar casein composition were produced. These dairy systems were based on two different protein milk concentrates produced using either Microfiltration (MF) or Ultrafiltration (UF) processes.

2.1.1. MF concentrate

The aim of the membrane filtration process developed in this study was to obtain an almost pure casein concentrate, dispersed in the same aqueous phase of milk, in order to mimic as much as possible the protein composition of a real cheese. Skim milk (Entremont, Montauban de Bretagne, France) was initially filtered to remove contaminating bacteria using the microfiltration pilot equipment GP7 fitted with a 0.8 μm Sterilox GP membrane. This microfiltrate was then concentrated by microfiltration using a 0.1 μm aluminum Zircone membrane. This smaller pore size allowed the concentration of the casein fraction only, the size of the whey proteins in milk being sufficiently small to cross the membrane. In order to increase the concentration factor of the caseins, it was necessary to proceed to a diafiltration step of the concentrate, using the MF permeate instead of water in order to keep the same aqueous phase of milk in the final concentrate. The permeate had been previously ultrafiltrated with a 5 kD membrane to remove the whey proteins. The overall filtration process allowed concentrating the total proteins of milk by a factor of 4.3. Neither NaCl nor cream was added, leaving a non-salty and a non-fatty MF concentrate. The composition of the MF concentrate (pH 6.6) is given in Table 1.

2.1.2. UF concentrate

The UF concentrate was produced following previously described procedures (Ulve et al., 2008; Silva, Peixoto, Lortal, & Floury, 2013). Unlike microfiltration, the ultrafiltration process allowed the concentration of all the proteins of milk, both the caseins and the whey proteins. This UF concentrate has then the same protein composition as for some commercial cheeses obtained by using the MMV technology, such as Pavé d'Affinois (Maubois, Mocquot, & Vassal, 1969; Maubois & Mocquot, 1971; Maubois & Mocquot, 1975). Overall, the total proteins of milk were concentrated in this case by a factor of 5. Once again, neither NaCl nor

177 cream was added, leaving a non-salty and a non-fatty UF concentrate. The composition of the
178 UF concentrate (pH 6.6) is given in Table 1.

179 The MF concentrate was used without further preparation whereas the UF concentrate
180 was heated at 93°C for 15 min (Aly et al., 2011) and then cooled using melting ice for 3 min.
181 Sodium azide was added to both the MF and heat-treated UF concentrates at a final
182 concentration of 0.05% (wt/wt) in order to prevent microorganism growth. About 1 mL of the
183 MF concentrate or of the heat-treated UF concentrate were poured into 2 mL Eppendorf tubes
184 and then incubated at 30°C for 1 h and then held at 19°C for 2 h to obtain the MF-suspension
185 or the UF-suspension, respectively. Both suspensions were passively aspired by using
186 cellulose microcapillary tubes with a 200 µm inner diameter ahead of further preparation for
187 TEM.

188 The concentrated milk gels were produced from the same concentrates (i.e.; MF or
189 heat-treated UF concentrates). In this case, after adding sodium azide to the concentrates
190 (0.05% wt/wt), the coagulant agent Maxiren 180 (DSM Food Specialties, Seclin, France) was
191 added giving a final concentration of 0.03% (v/v). After homogenization, 600 µL of each
192 mixture (MF or heat-treated UF concentrate + coagulant agent) was slowly poured into mini-
193 gel cassette® systems (IFR Norwich, U.K.), containing flat gold-plated specimen carriers (0.5
194 mm thick, 1.5 mm in diameter, 200 µm deep; Leica Cat #16706898). The gel cassettes®
195 systems were incubated at 30°C for 1 h to enable coagulation and then at 19°C for 2 h to
196 obtain the final gels based on each concentrate.

197

198 *2.2. Transmission electron microscopy*

199

200 The prepared concentrated milk suspensions and gels were frozen using a Leica EM
201 PACT2 high-pressure freezer (Leica Microsystems, Vienna, Austria). The sample carriers,

cellulose microcapillary tubes or flat gold-plated specimen carriers, were pre-coated with 1% phosphatidylcholine (Sigma-Aldrich Ltd.) diluted in chloroform to avoid sample sticking. No cryo-protecting agent was added to the samples. For the freeze-substitution step, Leica EM AFS2 freeze substitution machine (Leica Microsystems, Vienna, Austria) was used. The frozen samples were transferred in liquid nitrogen to a processing container equipped with a flat spacer (Leica Microsystems, Vienna, Austria). The frozen samples were freeze-substituted in 2% osmium tetroxide diluted in anhydrous acetone. After an initial incubation of 8h at -90°C the temperature was gradually (5°C/hour) raised to -30°C and samples were then left for another 8h at this temperature. The solvent-fixative solution was replaced with pre-chilled mix of ethanol 3:1 resin (epon-araldite mix; Sigma-Aldrich Ltd). The temperature was then gradually brought up to room temperature and further ethanol:resin substitutions were done following the resin manufacturer instructions. Thin sections (90 nm) of embedded samples were cut with a diamond knife using a Reichert ultramicrotome. The sections were contrasted with 4% aqueous solution of uranyl acetate and observed using a JEM-1400 Transmission Electron Microscope (JEOL Ltd., Tokyo, Japan) operated at 120 kV accelerating voltage. Digital images were acquired using the Gatan SC1000 Orius® CCD camera (4008 x 2672), set up with the imaging software Gatan DigitalMicrograph™ (Gatan, Pleasanton, USA).

Several TEM micrographs were taken on different parts of two independent samples of each of the four dairy systems. Ten micrograph images were chosen independently for each dairy system for further image analysis.

The resulting images each represented an area of 9.97 x 6.64 μm and showed the microstructure of the samples at a magnification of x20000. Images were saved as 32-bit grayscale dm3 images of 4008 x 2670 pixels (where 1 pixel = 2.5 nm).

227 *2.3. Image processing of TEM micrographs*

228

229 Several image processing steps were necessary to automatically segment the TEM
230 images of the four dairy systems (concentrated milk suspensions and gels). These steps are
231 schematically set out in Fig. 1. Each image was normalized using a blank background image
232 (obtained without sample or resin) (Fig. 1B). This permitted the removal of intensity
233 variations over the image. Histogram normalization procedure was applied and the result was
234 converted to images based on 256 shades of gray (Fig. 1C). As artifacts could be detected on
235 some micrographs, they were removed by applying a "black top-hat" operation with a square
236 structuring element of 200x200 pixels (Fig. 1D). Black top-hat is a tool (taken from
237 mathematical morphology) that enhances dark structures smaller than the chosen structuring
238 element while removing larger variations (Soille, 2003). A smoothing operator was then
239 applied (by computing the average of pixel values in a circular neighborhood with radius of
240 10 pixels) to remove the acquisition noise (Fig. 1E). The two phases were contrasted, with
241 images histograms showing two peaks (Fig. 1F). "Otsu automated threshold" is commonly
242 used for the segmentation of dairy product images (Ong et al., 2011; Hussain, Grandison, &
243 Bell, 2012; Impoco et al., 2006) and was used for the segmentation in the present study. Otsu
244 threshold consists in identifying the threshold value that best discriminates between the two
245 phases, by minimizing the intra-class variance while maximizing inter-class variance (Otsu,
246 1979). The segmentation procedure was validated by visual inspection of the binary images
247 superimposed on the original images.

2.4. Quantification of microstructural parameters

The values of the microstructural parameters determined in the present work may depend on several factors such as sample thickness and image processing (i.e., filter choice, segmentation threshold). Therefore, the proposed image analysis procedure was first validated by comparing microstructural parameters of concentrated milk suspensions with those of both synthetic images and data taken from the literature. Finally, the values of microstructural parameters obtained for the different dairy systems in the same conditions could be compared between them.

2.4.1. Generation of synthetic images of a suspension

In order to validate and help to interpret microstructural parameters, the developed image analysis method was applied on synthetic images mimicking a theoretical suspension of micelles. A set of non-overlapping balls was generated in a 3D cuboid with dimensions 5x5x2 µm. The diameter of the balls was chosen as 120 nm, corresponding to the mean diameter of casein micelles (Fox & Brodkorb, 2008). In order to avoid edge effects, a margin of 200 nm was applied on all sides. The number of balls was chosen to have a numerical density equal to 160 micelles/µm ^{3}, corresponding to an expected number of 8000 within the cuboid. This value was chosen to generate an area fraction in the synthetic images similar to the one observed for milk suspensions in the present study. To avoid overlap, a minimal distance of 130 nm was imposed between the micelle centers. The physical cut was represented by a horizontal slice with thickness 90 nm, and located in the middle of the cuboid. An example of a synthetic suspension of micelles is shown on Fig. 2A. The intersection of the slice with the set of balls was used to generate a planar binary image representing a virtual observation of the model system. A resolution of 2.5 nm by pixel was

used, resulting in a 2000x2000 pixels binary image (Fig. 2B). Ten images were thus generated to address the variability of measurement method. Due to the thickness of the slice, some micelles seemed to overlap, seemingly forming small agglomerates. Other micelles present a smaller section because they were not located within the sampled slice. Matlab software was used both to simulate the 3D synthetic suspensions and to generate the corresponding binary images (Mathworks, Natick, MA). The Free-D software was used to produce the sample image of Fig. 2A (Andrey & Maurin (2005), http://free-d.versailles.inra.fr/html/freed.html).

2.4.2. Global morphometry

Global morphometry was used to determine three global microstructural parameters: area fraction, porosity, and boundary length per unit area. If the sampling slice can be assumed to have a small thickness relative to size of the structures, these parameters can be directly related to 3D properties of the network by using stereological relations.

Area fraction was defined as the ratio between dark area (i.e.; the protein matrix) with respect to the total area of the image. The dark area corresponds to the area covered by particles (for suspensions) or by particle aggregates (for gels) in the micrograph cross-sections. Porosity is the complementary parameter and can be defined as the division of the void area by the total image area. In the binary image, porosity was calculated as white area (free space, corresponding to the aqueous phase) as a percentage of the total area (Impoco et al., 2006; Rovira et al., 2011).

The boundary length per unit area is the length of the perimeter around all the particle edges or boundaries (for suspensions) or particle aggregate edges or boundaries (for gels), divided by the total image area. The boundary length per unit area thus measures the quantity of interface between the protein phase and the aqueous phase. For a comparable area density, its value will be larger for systems with small structures and/or tortuous interfaces, and

298 smaller for systems with large structures and/or smooth interfaces. Boundary length was
299 estimated by using a discretized version of Crofton formula, which consists in counting the
300 number of intercepts with lines of various orientations, and normalized by the area of the
301 image (Ohser & Mücklich, 2000; Legland, Kiêu, & Devaux, 2007).
302
303 *2.4.3. Image morphological granulometry*
304 The typical size of particles (or particle aggregates) and inter-particle (or inter-particle
305 aggregate) distances were determined by applying binary image granulometry on the
306 segmented images. Binary image granulometry is based on image transformations depending
307 on the size of a mask referred to as a "structuring element". One of the basic transformations
308 (taken from mathematical morphology) is the morphological opening, which effectively
309 removes objects smaller than the structuring element (Soille, 2003). By applying openings of
310 increasing sizes to the dairy system images, the particles (or particle aggregates) are
311 progressively removed. The complementary transformation is morphological closing, which
312 effectively makes the voids smaller than the defined structuring element disappear. Following
313 the same process, applying closings of increasing size to the images leads to a progressive
314 elimination of the part of the image showing the voids in the structure. Thus, by either
315 method, a particle (or void) size distribution curve is produced.
316 The curve *V(i)* is generated by counting the number of pixels after each closing or
317 opening step. This is then normalized according to the initial and final number of pixels
318 *V(initial)* and *V(final)* and the finite difference is computed to build a granulometric curve:
319

$$g(i) = \frac{V(i) - V(i+1)}{V(initial) - V(final)} \quad (1)$$

320

In the current study, the largest size (diameter) of the disk structuring element was 121 pixels, corresponding to about 300 nm on the image. To reduce computation time, structuring element diameters were considered with a step of 4 pixels. To compare granulometric curves for a set of samples, each granulometric curve was summarized by computing its geometric mean. The following weighted sum was used:

$$m = exp\left(\sum_{i=1}^{imax} g(i) * \log(t_i)\right) \quad (2)$$

where *g(i)* is the percent of grey level variation for the step *i*, t_i is the size of the structuring element in µm and *imax* is the number of closing/opening steps (Legland, Devaux, Bouchet, Guillon, & Lahaye, 2012). The geometric means of the granulometric curves obtained with the openings procedure were interpreted as the average size of particles (for suspensions) or particle aggregates (for gels). The geometric means of the granulometric curves obtained with the closings procedure were interpreted as the average size of the aqueous phase between the particles or particle aggregates.

A schematic representation of microstructural parameters determined for suspensions and gels by using the image morphological granulometry method is given in Fig. 3.

2.4.4. Tortuosity

The tortuosity in every point in the aqueous phase can be defined as the ratio of the shortest path (i.e.; avoiding the protein network) between two opposing borders of the image, over the Euclidean distance between the same borders (Delarue & Jeulin, 2003; Wu et al., 2006). An illustration of the tortuosity for a sample structure is given in Fig. 4. The 3D tortuosity cannot be determined from 2D images, but 2D tortuosity can be used to

quantitatively compare the microstructure of different dairy systems observed under similar conditions.

For points belonging to aqueous phases totally included in the protein network, no path can be defined to image borders. Consequently, the tortuosity over an image was defined as the average value measured at points for which shortest paths could be computed. As the length of the shortest path is always greater than the Euclidean distance, the tortuosity is always greater than or equal to one. The tortuosity value increases with the complexity of the protein network separating the aqueous phase.

In order to assess the variability of the tortuosity measurement, each image was divided into four sub-images, and tortuosity was calculated for each sub-image. For most images, the tortuosity of the complete image was similar to the average value of the sub-images (the difference being less than the standard deviation). However, for some images, the difference was greater, due to large blocks of protein network that introduce a large variability in the measurement.

2.5. Software implementation

Image processing and analysis was performed using Fiji-win64 processing software. The quantification of morphological features required the development of specific plugins, which are available on request from the authors, or from the Internet at http://www.pfl-cepia.inra.fr/index.php?page=ijGranulometry_en, http://www.pfl-cepia.inra.fr/index.php?page=ijGeodesics_en, http://www.pfl-cepia.inra.fr/index.php?page=imMinkowski_en.

369 *2.6. Statistical Analysis*

370

371 The mean values of microstructural parameters obtained for the four different dairy
372 systems studied (MF-suspension, UF-suspension, MF-gel and UF-gel) were statistically
373 compared using R software (version R i386 3.0.2) (R Foundation for Statistical Computing,
374 Vienne, Austria). Results are presented with the mean value and the standard deviation. One-
375 way analysis of variance (ANOVA) and Tukey's paired comparison test were applied in order
376 to determine which means are significantly different from one another at the 95% family-wise
377 confidence level. The Student's test was applied in order to compare the two suspensions and
378 the two gels.

379

380 **3. Results and Discussion**

381

382 *3.1. Image processing of TEM micrographs*

383

384 Sample images of TEM acquisition obtained by using the HPF-FS protocol are
385 presented in Fig. 5, for both pairs of suspensions and gels. The dark phase corresponds to the
386 protein matrix (i.e.; particles or particle aggregates). The lighter phase corresponds to the
387 aqueous phase, formed by water, lactose, minerals and free amino acids. In all dairy systems,
388 the particles and particle aggregates were homogeneously distributed.

389 The particle aggregates observed in the gels (Fig. 5C and 5D) are larger compared to
390 the individual particles in suspensions (Fig. 5A and 5B).

391 Representative segmented TEM micrographs of the concentrated milk suspensions and
392 gels are illustrated in Fig. 6. These segmented images correspond to the TEM micrographs
393 shown in Fig. 5. The black phase of the segmented micrographs corresponds to the protein

matrix (i.e.; particles or particle aggregates), while the white phase corresponds to the aqueous phase.

3.2. Quantification of microstructural parameters

3.2.1. Validation of the automated image analysis procedure

Microstructural parameters were measured for the two concentrated milk suspensions in order to validate the image processing of TEM micrographs by comparing with values taken from the literature. Obtained values were also compared to those obtained on synthetic suspension images. Table 2 presents the values of the microstructural parameters obtained from TEM micrographs of the milk suspensions.

Area fractions measured from TEM micrographs were equal to 0.34 ± 0.02 and 0.33 ± 0.01 for the MF- and UF-suspensions, respectively. Area fractions did not differ statistically ($p < 0.05$) between the MF- and UF-suspensions. This fact can be explained by the same casein concentration in both suspensions (130 g/kg).

The number of micelles in the synthetic suspension image was adjusted to obtain a value of area fraction similar to that for the real suspensions. The related value for the synthetic images was equal to 0.338 ± 0.005. The other microstructural parameters can therefore be compared between synthetic and real suspensions.

The mean particle size obtained by granulometry on the synthetic suspension images was estimated as 116.3 ± 0.3 nm. This is very close to the diameter of the casein micelles, validating the image analysis method in this respect. Nonetheless, the measured values on the synthetic suspension images were still smaller than the real diameter of casein micelles, which is attributed to the presence of smaller sections of micelles.

418 Fig. 7 shows granulometric curves for the milk suspensions representing the particle
419 size distribution (Fig. 7A and 7B for MF- and UF-suspensions, respectively) and the
420 distribution of inter-particle distances (Fig. 7C and 7D for MF- and UF-suspensions,
421 respectively). A good repeatability of the particle size distributions and of inter-particle
422 distance is noted for both MF- and UF-suspensions. The corresponding mean particle size and
423 inter-particle distance values from the geometric means are given in Table 2.

424 The mean particle size was 88 ± 3 nm and 99 ± 4 nm for the MF- and UF-suspensions.
425 At the casein concentration used (130 g/kg, corresponding to ~140 g/L for these suspensions),
426 casein micelles are fully separated from each other, i.e., below the concentration of random-
427 close packing estimated as ~178 g/L (Bouchoux, Debbou, Gésan-Guiziou, Famelart, &
428 Doublier, 2009). Casein micelles present in milk are known to have a broad size distribution
429 with diameters ranging from 50 to 500 nm, and a mean diameter of ~120 nm (Fox &
430 Brodkorb, 2008). The values obtained by image analysis fall within this range of diameters
431 found for casein micelles in unconcentrated milk, but are smaller than the indicated mean
432 diameter. Similar results were reported by Srilaorkul et al. (1991), who studied the effect of
433 skim milk ultrafiltration on particle size using conventional TEM. They measured particle size
434 by observation using a Baush and Lomb measurement magnifier, counting and classifying the
435 micelles into 10 classes, each with a width of 20 nm. They saw a decrease in mean casein
436 micelle diameter from 118 nm in normal milk to 87 nm in milk that had been concentrated
437 five times. The change in the composition of casein and minerals as a result of the
438 ultrafiltration of milk may be responsible for the change in average diameter of the casein
439 micelles.

440 The UF-suspension presented a mean particle size greater than that for the MF-
441 suspension. The larger mean particle size (of about 10 nm) for the UF-suspension may be due
442 to the association of denatured whey proteins on the surface of the micelles due to the heat

443 treatment applied to the UF concentrate (Jeurnink & de Kruif, 1993; Anema & Li, 2003; Nair,
444 Dalgleish, & Corredig, 2013). Anema & Li (2003) demonstrated that the diameter of casein
445 micelles in heated reconstituted skim milk increased by 19 nm as a consequence of heat
446 treatments. For the concentrated milk studied in the same work, prepared by subjecting milk
447 to a combination of ultrafiltration and microfiltration techniques, an overall increase of 5 nm
448 was observed when samples at pH 6.55 were heated for 45 min at 90°C. These values are
449 comparable to the increase of about 10 nm of mean particle size found in the current study for
450 the (heat-treated) UF-suspension.

451 The mean inter-particle distance obtained from the image analysis was 123 ± 5 nm and
452 132 ± 2 nm for the MF- and UF-suspensions, respectively. These values are smaller than
453 those predicted from the synthetic suspension (153 ± 3 nm). This may be explained by the
454 differences in the diameter distribution: as real suspensions contain a larger number of small
455 micelles the mean free distance will be less. The mean free distance between casein micelles
456 in unconcentrated milk is reported as around 240 nm (Fox & Brodkorb, 2008). As expected,
457 the mean inter-particle distances between the casein micelles would be smaller in the
458 concentrated milk suspensions than in milk (25 g/L) due to the higher casein concentration
459 (130 g/kg, i.e. around 140 g/L) as a result of the membrane technology (microfiltration or
460 ultrafiltration processes) applied. It is known that when the concentration of total solids in
461 skim milk increases (e.g. during ultrafiltration), the distance between the casein micelles
462 decreases due to the increased volume fraction (Karlsson, Ipsen, Schrader, & Ardö, 2005).

463 The images of the MF- and UF-suspensions presented similar area fraction values
464 whereas the particle size and inter-particle distance values were statistically different. The
465 mean inter-particle distance was greater for the UF-suspension (when compared with the MF-
466 suspension) that counteracted, to some extent, the effect of the larger mean particle size.

The MF-suspension images presented a boundary length per unit area of 13.3 ± 0.5 μm/μm^2, and the UF-suspension a value of 12.1 ± 0.2 μm/μm^2. This parameter is a measure of the quantity of interface between the protein phase (black phase) and the aqueous phase (white phase). For comparison, the values measured for the synthetic suspension images were 11.5 ± 0.2 μm/μm^2. This may be explained by the fact that synthetic suspensions are more regular than real ones. The value was significantly larger for the MF-suspension than for the UF-suspension. This result may have been expected because a suspension with small particles (MF-suspension) will have a greater interface (between the particles and the aqueous phase) and thus a larger boundary length per unit area value. As both suspensions have the same area fraction, the observed difference depends on the regularity of the interface. Assuming a suspension of spherical particles, an interpretation is that the MF-suspension is composed of smaller particles compared with the UF-suspension.

The tortuosity was 1.08 ± 0.01 for the MF-suspension and 1.06 ± 0.01 for the UF-suspension. These values were not significantly different ($p < 0.05$) but they were a little bit larger than that for the synthetic suspensions (1.043 ± 0.001). It can be observed that tortuosity value increases when mean distance between micelles decreases, and when boundary length per unit area increases.

Overall, the microstructural parameter values predicted for concentrated milk suspensions by the image analysis procedure were in agreement with literature findings and also with results obtained for a synthetic suspension. This fact allowed us to validate the image processing of TEM micrographs.

3.2.2. Application of the automated image analysis procedure to milk gels

The image analysis procedure validated previously for the two types of concentrated milk suspensions was then applied to their corresponding gels, which had been obtained by rennet-induced coagulation, in order to determine their microstructural parameters.

The microstructure of milk gels is more complex than that for suspensions and depends on several factors such as the type of coagulation and the treatment applied to the milk concentrate prior to the coagulation step. It is well known that the addition of chymosin cleaves a specific bond of the κ-casein on the surface of the micelles. This reduces the steric and electrostatic repulsion between the micelles, and the destabilized micelles thus begin to aggregate to form the gel (Mellema, Heesakkers, van Opheusden, & van Vliet, 2000).

Table 3 sets out the values for the microstructural parameters obtained from the TEM images of MF- and UF-gels.

The mean area fractions were 0.49 ± 0.03 and 0.50 ± 0.02 for MF- and UF-gels, respectively, which were significantly ($p < 0.05$) larger than the values obtained for the related suspensions (0.34 ± 0.02 and 0.33 ± 0.01 for MF- and UF-suspensions, respectively). However, similar area fraction values should be expected for concentrated milk suspensions and gels presenting the same casein concentration. This unexpected result may be explained by the aggregation of casein micelles in the gel which could induce changes in the apparent density of particles on the TEM images, due to the slice thickness of the sample.

Curds from heat-treated milks tend to be weak, ragged in appearance with a poor matting ability and poor fusion of the gel network, giving rise to more porous matrices (Singh & Waungana, 2001). However, in the present study, the UF-gel (made from heat-treated UF concentrate) presented the same porosity compared with the MF-gel (about 0.50). This fact can be explained by the ultrafiltration of the milk prior to coagulation in the case of the UF-gel. It is known that gels formed from UF concentrates are much firmer than the

517 corresponding curds produced from unconcentrated milks at comparable levels of β-
518 lactoglobulin denaturation and association (Singh & Waungana, 2001). This result is
519 interesting because gels obtained from different technological treatments but with the same
520 casein composition have a similar porosity. Thus, heat treatment in combination with
521 concentration processes such as ultrafiltration may yield opportunities to correct curd
522 properties.

523 Fig. 8 shows granulometric curves obtained by applying the opening procedure (Fig.
524 8A and 8B for MF- and UF-gels, respectively), representing the distribution of particle
525 aggregate sizes and by the closing procedure (Fig. 8C and 8D for MF- and UF-gels,
526 respectively), representing the distribution of inter-particle aggregate distances obtained from
527 TEM micrographs. Fig. 8 demonstrates the good repeatability of the distribution of particle
528 aggregate size and inter-particle aggregate distance values obtained from different TEM
529 micrographs of the MF- and UF-gels. Values for these same parameters are set out in Table 3.

530 The MF-gel exhibited a mean particle aggregate size of 141 ± 3 nm, slightly larger
531 than the mean particle aggregate size in UF-gel, 135 ± 8 nm. Concerning the rennet-induced
532 gels, it is known that in milk that has been heated, the κ-casein is broken down by chymosin
533 (as it is in unheated milk), but that the micelles do not aggregate well (Kethireddipalli, Hill, &
534 Dalgleish, 2011). This is due to the presence of denatured whey proteins on the micellar
535 surface, which may hinder the close approach of the potentially interacting sites on the
536 micelles (Dalgleish & Corredig, 2012). Waungana, Singh, & Bennett (1996) observed that the
537 denaturation of individual whey proteins and their association with the casein micelles
538 resulted in prolonged gelation times and reduced gel firmness in gels produced from heat-
539 treated UF milk (UHT system; 80°C to 140°C for 4s) due to the formation of a limited
540 number of reactive sites at the micellar surface. It may thus follow that the denatured whey
541 proteins associated on the micellar surface in the UF concentrate prevented the close approach

542 of casein micelles, resulting in smaller particle aggregates in the (heat-treated) UF-gel when
543 compared with the MF-gel.

544 As expected, the mean particle aggregate size is larger in the two gels studied
545 compared with the mean particle size in the corresponding suspensions. This may be
546 explained by the aggregation of casein micelles in gels as a consequence of the addition of the
547 coagulant agent (rennet) (Walstra, Bloomfield, Jason Wei, & Jenness, 1981).

548 Mean inter-particle aggregate distances were shown by image analysis as 147 ± 5 nm
549 for the MF-gel, significantly greater than the mean value of 131 ± 7 nm obtained for the UF-
550 gel. The MF-gel contained particle aggregates and inter-particle aggregate distances greater
551 than those found in the UF-gel. These results are consistent with the boundary length unit area
552 values obtained for these gels.

553 The boundary length per unit area for the UF-gel was 10.7 ± 0.7 $\mu m/\mu m^2$, significantly
554 larger ($p < 0.05$) than the value found for the MF-gel, 9.5 ± 0.3 $\mu m/\mu m^2$. The boundary length
555 per unit area values obtained for the gels were larger when the particle aggregate sizes were
556 smaller (Table 3). This result was expected because matrices with smaller particle aggregates
557 present more interfaces (particle aggregates/aqueous phase).

558 Values of boundary length per unit area were significantly larger ($p < 0.05$) in the gels
559 when compared to suspensions. This result was also expected because particle sizes in
560 suspensions were found to be significantly smaller ($p < 0.05$) than particle aggregate sizes in
561 gels. Therefore, in suspensions, more interfaces (particle/aqueous phase) were present,
562 resulting in bigger values of boundary length per unit area values.

563 Tortuosity values were similar for the two concentrated milk gels (1.5 ± 0.2 and 1.5 ±
564 0.2 for MF- and UF-gels, respectively). These values are much larger than for the
565 suspensions. This corresponds to the increase in the aggregate size, which leads to longer

paths between given points. In this study, the tortuosity value could not enable discrimination between different gel microstructures but with similar casein composition.

4. Conclusions

An automated image analysis procedure for microstructural characterization of dairy systems was developed. The procedure was first applied to models of synthetic suspensions, and then on milk suspensions (with comparison with published data) to validate the methodology. The computerized image analysis method enabled an easy measurement of a series of microstructural parameters of milk gels, which makes it especially useful for routine measurements.

The measurements of the area fraction (and hence of the sample porosity) were similar for the MF- and UF-suspensions, and for the MF- and UF-gels. The image analysis procedure made it possible to quantify differences of microstructure independently of the area fraction. Binary image granulometry measures particle size distribution that can also be represented by an average particle size. In a similar way, the distribution of distances between particles can be represented by an average value. These two measurements can describe dairy systems by using parameters that can be easily interpreted and compared.

The measurement of boundary length per unit area indicates the complexity of the matrix microstructure, without making the assumption that the system is a collection of particles. In case of particles systems with a similar area fraction, this parameter seems to be correlated with the average particle size.

The tortuosity of a sample describes the complexity of the aqueous phase, and is expected to be related to diffusion properties. In this study, the measured values were different for suspensions and gels, but no difference could be discerned between the two gels

studied (obtained with different preparation methods). Tortuosity is difficult to measure when the area fraction of the solid phase is large: when the aggregates are large, the probability of observing non-connected aqueous phases increases. An alternative could be to allow the computation of geodesic distances in both phases but using different propagation speeds (Wu et al., 2006), or to consider the tortuosity over a limited distance.

It was demonstrated that the image analysis method for the estimation of microstructural parameters was able to differentiate between dairy systems of similar composition, but obtained from different processes.

For a better understanding of the microstructure of dairy systems, modeling approaches might be considered. In this study, we have simulated binary images similar to suspension images, with the objective of validating the image analysis methodology. However, the microstructure of milk gels is much more complex and involves a variety of physical and chemical processes. Several modeling approaches have already been undertaken by other authors to reconstruct the microstructure based on 2D or 3D observations (Yeong & Torquato, 1998; Kumar, Briant, & Curtin, 2006; Nisslert, Kvarnström, Loren, Nyden, & Rudemo, 2007; Jiang, Chen, & Burkhart, 2013). Similar approaches could be investigated for dairy systems.

The developed image analysis procedure enables new insights into the characterization of the microstructure of dairy systems. This approach, which was applied to milk gels, might be adapted and extended to other food systems.

This procedure can also contribute to a better understanding of the effects of processing on the structure-property relationships in dairy products. For instance, further work might focus on coupling measurements obtained by image analysis, which describe the microstructure of milk gels, to physical phenomena such as diffusion properties.

Acknowledgments

The authors would like to thank Antoine Bouchoux (INSA, Toulouse, France) and Marie-Hélène Famelart (INRA, Rennes, France) for their help and suggestions during the writing of this paper. The authors also wish to thank the members of MRic TEM facility (Rennes, France) for their help with the TEM observations. The authors acknowledge with gratitude the financial support received both from the Brittany Regional Council and from INRA Rennes (France).

References

Aguilera, J. M., Stanley, D. W., & Baker, K. M. (2000). New dimensions in microstructure of food products. *Trends in Food Science & Technology, 11*(1), 3-9.

Aly, S., Floury, J., Famelart, M. H., Madec, M. N., Dupont, D., Le Gouar, Y. et al. (2011). Nisin quantification by ELISA allows the modeling of its apparent diffusion coefficient in model cheeses. *Journal of Agricultural and Food Chemistry, 59*(17), 9484-9490.

Andrey, P. & Maurin, Y. (2005). Free-D: an integrated environment for three-dimensional reconstruction from serial sections. *Journal of Neuroscience Methods, 145*(1–2), 233-244.

Anema, S. G. & Li, Y. (2003). Association of denatured whey proteins with casein micelles in heated reconstituted skim milk and its effect on casein micelle size. *Journal of Dairy Research, 70*, 73-83.

Bouchoux, A., Debbou, B., Gésan-Guiziou, G., Famelart, M.-H., & Doublier, J.-L. (2009). Rheology and phase behavior of dense casein micelle dispersions. *The Journal of Chemical Physics, 131*(16).

Büchheim, W. (1982). Aspects of sample preparation for freeze-fracture/freeze-etch studies of proteins and lipids in food systems: a review. *Food Microstructure, 1*(2), 189-208.

Crossley, J. I. & Aguilera, J. M. (2001). Modeling the effect of microstructure on food extraction. *Journal of Food Process Engineering, 24*(3), 161-177.

Dalgleish, D. G. & Corredig, M. (2012). The structure of the casein micelle of milk and its changes during processing. *Annual Review of Food Science and Technology, 3*(1), 449-467.

Delarue, A. & Jeulin, D. (2003). 3D morphological characterization of composite materials with spherical aggregates. *Image Analysis and Stereology, 22*, 153-161.

El-Bakry, M. & Sheehan, J. (2014). Analysing cheese microstructure: A review of recent developments. *Journal of Food Engineering, 125*, 84-96.

651 Ercili-Cura, D., Lille, M., Legland, D., Gaucel, S., Poutanen, K., Partanen, R. et al. (2013).
652 Structural mechanisms leading to improved water retention in acid milk gels by use of
653 transglutaminase. *Food Hydrocolloids, 30*(1), 419-427.

654 Fallico, V., Tuminello, L., Pediliggieri, C., Horne, J., Carpino, S., & Licitra, G. (2006).
655 Proteolysis and microstructure of Piacentinu Ennese cheese made using different farm
656 technologies. *Journal of Dairy Science, 89*(1), 37-48.

657 Fenoul, F., Le Denmat, M., Hamdi, F., Cuvelier, G., & Michon, C. (2008). Technical Note:
658 Confocal Scanning Laser Microscopy and quantitative image analysis: Application to
659 cream cheese microstructure investigation. *Journal of Dairy Science, 91*(4), 1325-
660 1333.

661 Fox, P. F. & Brodkorb, A. (2008). The casein micelle: Historical aspects, current concepts and
662 significance. *International Dairy Journal, 18*(7), 677-684.

663 Fucà, N., Pasta, C., Impoco, G., Caccamo, M., & Licitra, G. (2013). Microstructural
664 properties of milk fat globules. *International Dairy Journal, 31*(1), 44-50.

665 Geng, X. L., van den Berg, F. W. J., Bager, A. N., & Ipsen, R. (2011). Dynamic visualization
666 and microstructure of syneresis of cheese curd during mechanical treatment.
667 *International Dairy Journal, 21*(9), 711-717.

668 Goff, H. D., Verespej, E., & Smith, A. K. (1999). A study of fat and air structures in ice
669 cream. *International Dairy Journal, 9*(11), 817-829.

670 Gunasekaran, S. & Ding, K. (1999). Three-dimensional characteristics of fat globules in
671 cheddar cheese. *Journal of Dairy Science, 82*(9), 1890-1896.

672 Hussain, I., Grandison, A. S., & Bell, A. E. (2012). Effects of gelation temperature on
673 Mozzarella-type curd made from buffalo and cows milk. 1: Rheology and
674 microstructure. *Food Chemistry, 134*(3), 1500-1508.

675 Impoco, G., Carrato, S., Caccamo, M., & Tuminello, L. (2006). Quantitative analysis of
676 cheese microstructure using SEM imagery. In *SIMAI 2006 Minisymposium: Image*
677 *Analysis Methods for Industrial Application*.

678 Impoco, G., Fucà, N., Pasta, C., Caccamo, M., & Licitra, G. (2012). Quantitative analysis of
679 nanostructures shape and distribution in micrographs using image analysis. *Computers*
680 *and Electronics in Agriculture, 84*, 26-35.

681 Jeurnink, T. J. M. & de Kruif, K. G. (1993). Changes in milk on heating: viscosity
682 measurements. *Journal of Dairy Research, 60*(2), 139-150.

683 Jiang, G. Z., Chen, W., & Burkhart, C. (2013). Efficient 3D porous microstructure
684 reconstruction via Gaussian random field and hybrid optimization. *Journal of*
685 *Microscopy, 252*(2), 135-148.

686 Kalab, M., Allan-Wojtas, P., & Mistry, V. V. (1995). Microscopy and other imaging
687 techniques in food structure analysis. *Trends in Food Science & Technology, 6*, 3210-
688 3218.

689 Karlsson, A. O., Ipsen, R., Schrader, K., & Ardö, Y. (2005). Relationship between physical
690 properties of casein micelles and rheology of skim milk concentrate. *Journal of Dairy*
691 *Science, 88*(11), 3784-3797.

692 Kethireddipalli, P., Hill, A. R., & Dalgleish, D. G. (2011). Interaction between casein micelles
693 and whey protein/kappa-casein complexes during renneting of heat-treated
694 reconstituted skim milk powder and casein micelle/serum mixtures. *Journal of*
695 *Agricultural and Food Chemistry, 59*(4), 1442-1448.

696 Kumar, H., Briant, C. L., & Curtin, W. A. (2006). Using microstructure reconstruction to
697 model mechanical behavior in complex microstructures. *Mechanics of Materials,*
698 *38*(8–10), 818-832.

699 Lanfrey, P. Y., Kuzeljevic, Z. V., & Dudukovic, M. P. (2010). Tortuosity model for fixed
700 beds randomly packed with identical particles. *Chemical Engineering Science, 65*(5),
701 1891-1896.

702 Latour, L. L., Kleinberg, R. L., Mitra, P. P., & Sotak, C. H. (1995). Pore-size distributions and
703 tortuosity in heterogeneous porous media. *Journal of Magnetic Resonance, Series A,*
704 *112*(1), 83-91.

705 Le Feunteun, S. & Mariette, F. (2007). Impact of casein gel microstructure on self-diffusion
706 coefficient of molecular probes measured by ^{1}H PFG-NMR. *Journal of Agricultural*
707 *and Food Chemistry, 55*(26), 10764-10772.

708 Le Feunteun, S. & Mariette, F. (2008). PFG–NMR techniques provide a new tool for
709 continuous investigation of the evolution of the casein gel microstructure after
710 renneting. *Macromolecules, 41*(6), 2071-2078.

711 Legland, D., Devaux, M. F., Bouchet, B., Guillon, F., & Lahaye, M. (2012). Cartography of
712 cell morphology in tomato pericarp at the fruit scale. *Journal of Microscopy, 247*(1),
713 78-93.

714 Legland, D., Kiêu, K., & Devaux, M. F. (2007). Computation of Minkowski measures on 2D
715 and 3D binary images. *Image Analysis and Stereology, 26*(6), 83-92.

716 Lucey, J. A. (2002). Formation and physical properties of milk protein gels. *Journal of Dairy*
717 *Science, 85*(2), 281-294.

718 Marchesseau, S., Gastaldi, E., Lagaude, A., & Cuq, J. L. (1997). Influence of pH on protein
719 interactions and microstructure of process cheese. *Journal of Dairy Science, 80*(8),
720 1483-1489.

721 Maubois, J. L. & Mocquot, G. (1971). Préparation de fromage à partir de "pré-fromage
722 liquide" obtenu par ultrafiltration du lait. *Lait, 51*(508), 495-533.

723 Maubois, J. L. & Mocquot, G. (1975). Application of membrane ultrafiltration to preparation
724 of various types of cheese. *Journal of Dairy Science, 58*(7), 1001-1007.

725 Maubois, J. L., Mocquot, G., & Vassal, L. (1969). A method for processing milk and milk
726 products. [2052121]. French.

727 McMahon, D. J., Fife, R. L., & Oberg, C. J. (1999). Water partitioning in Mozzarella cheese
728 and its relationship to cheese meltability. *Journal of Dairy Science, 82*(7), 1361-1369.

729 McMahon, D. J. & McManus, W. R. (1998). Rethinking casein micelle structure using
730 electron microscopy. *Journal of Dairy Science, 81*(11), 2985-2993.

731 Mellema, M., Heesakkers, J. W. M., van Opheusden, J. H. J., & van Vliet, T. (2000).
732 Structure and scaling behavior of aging rennet-induced casein gels examined by
733 confocal microscopy and permeametry. *Langmuir, 16*(17), 6847-6854.

734 Morand, M., Guyomarc'h, F., Legland, D., & Famelart, M. H. (2012). Changing the
735 isoelectric point of the heat-induced whey protein complexes affects the acid gelation
736 of skim milk. *International Dairy Journal, 23*(1), 9-17.

737 Nair, P. K., Dalgleish, D. G., & Corredig, M. (2013). Colloidal properties of concentrated
738 heated milk. *Soft Matter, 9*(14), 3815-3824.

739 Nisslert, R., Kvarnström, M., Loren, N., Nyden, M., & Rudemo, M. (2007). Identification of
740 the three-dimensional gel microstructure from transmission electron micrographs.
741 *Journal of Microscopy, 225*(1), 10-21.

742 Ohser, J. & Mücklich, F. (2000). *Statistical analysis of microstructures in materials sciences*.
743 (1th ed.). Chichester: John Wiley & Sons.

744 Ong, L., Dagastine, R. R., Kentish, S. E., & Gras, S. L. (2011). Microstructure of milk gel and
745 cheese curd observed using cryo scanning electron microscopy and confocal
746 microscopy. *Food Science and Technology, 44*(5), 1291-1302.

747 Ong, L., Dagastine, R. R., Kentish, S. E., & Gras, S. L. (2012). The effect of pH at renneting
748 on the microstructure, composition and texture of Cheddar cheese. *Food Research*
749 *International, 48*(1), 119-130.

750 Ong, L., Dagastine, R. R., Kentish, S. E., & Gras, S. L. (2013). The effect of calcium chloride
751 addition on the microstructure and composition of Cheddar cheese. *International*
752 *Dairy Journal, 33*(2), 135-141.

753 Otsu, N. (1979). A threshold selection method from gray-level histograms. *IEEE Transactions*
754 *on Systems, Man, and Cybernetics, 9*(1), 62-66.

755 Ramasubramanian, L., Webb, R., D'Arcy, B., & Deeth, H. C. (2013). Characteristics of a
756 calcium–milk coagulum. *Journal of Food Engineering, 114*(2), 147-152.

757 Reis, P. J. M. & Malcata, F. X. (2011). Ripening-related changes in Serra da Estrela cheese: A
758 stereological study. *Journal of Dairy Science, 94*(3), 1223-1238.

759 Rovira, S., Lopez, M. B., Ferrandini, E., & Laencina, J. (2011). Hot topic: Microstructure
760 quantification by scanning electron microscopy and image analysis of goat cheese
761 curd. *Journal of Dairy Science, 94*(3), 1091-1097.

762 Sam Saguy, I., Marabi, A., & Wallach, R. (2005). New approach to model rehydration of dry
763 food particulates utilizing principles of liquid transport in porous media. *Trends in*
764 *Food Science & Technology, 16*(11), 495-506.

765 Shen, L. & Chen, Z. (2007). Critical review of the impact of tortuosity on diffusion. *Chemical*
766 *Engineering Science, 62*(14), 3748-3755.

767 Silva, J. V. C., Peixoto, P. D. S., Lortal, S., & Floury, J. (2013). Transport phenomena in a
768 model cheese: The influence of the charge and shape of solutes on diffusion. *Journal*
769 *of Dairy Science, 96*(10), 6186-6198.

770 Singh, H. & Waungana, A. (2001). Influence of heat treatment of milk on cheesemaking
771 properties. *International Dairy Journal, 11*(4–7), 543-551.

772 Smith, A. K., Kakuda, Y., & Goff, H. D. (2000). Changes in protein and fat structure in
773 whipped cream caused by heat treatment and addition of stabilizer to the cream. *Food*
774 *Research International, 33*(8), 697-706.

775 Soille, P. (2003). *Morphological Image Analysis: Principles and Applications*. (2 ed.).
776 Secaucus, NJ, USA: Springer-Verlag New York, Inc.

777 Srilaorkul, S., Ozimek, L., Ooraikul, B., Hadziyev, D., & Wolfe, F. (1991). Effect of
778 ultrafiltration of skim milk on casein micelle size distribution in retentate. *Journal of*
779 *Dairy Science, 74*(1), 50-57.

780 Suman, R. & Ruth, D. (1993). Formation factor and tortuosity of homogeneous porous media.
781 *Transp Porous Med, 12*(2), 185-206.

782 Torquato, S. (2002). *Random heterogeneous materials: microstructure and macroscopic*
783 *properties*. New York: Springer-Verlag.

784 Ulve, V. M., Monnet, C., Valence, F., Fauquant, J., Falentin, H., & Lortal, S. (2008). RNA
785 extraction from cheese for analysis of in situ gene expression of Lactococcus lactis.
786 *Journal of Applied Microbiology, 105*(5), 1327-1333.

787 Walstra, P., Bloomfield, V. A., Jason Wei, G., & Jenness, R. (1981). Effect of chymosin
788 action on the hydrodynamic diameter of casein micelles. *Biochimica et Biophysica*
789 *Acta (BBA) - Protein Structure, 669*(2), 258-259.

790 Waninge, R., Kalda, E., Paulsson, M., Nylander, T., & Bergenstahl, B. (2004). Cryo-TEM of
791 isolated milk fat globule membrane structures in cream. *Physical Chemistry and*
792 *Chemical Physics, 6*, 1518-1523.

793 Waninge, R., Nylander, T., Paulsson, M., & Bergenstahl, B. (2003). Milk membrane lipid
794 vesicle structures studied with cryo-TEM. *Colloids and Surfaces B: Biointerfaces,*
795 *31*(1-4), 257-264.

796 Waungana, A., Singh, H., & Bennett, R. J. (1996). Influence of denaturation and aggregation
797 of beta-lactoglobulin on rennet coagulation properties of skim milk and ultrafiltered
798 milk. *Food Research International, 29*(8), 715-721.

799 Wium, H., Pedersen, P. S., & Qvist, K. B. (2003). Effect of coagulation conditions on the
800 microstructure and the large deformation properties of fat-free Feta cheese made from
801 ultrafiltered milk. *Food Hydrocolloids, 17*(3), 287-296.

802 Wu, Y. S., van Vliet, L. J., Frijlink, H. W., & van der Voort Maarschalk, K. (2006). The
803 determination of relative path length as a measure for tortuosity in compacts using
804 image analysis. *European Journal of Pharmaceutical Sciences, 28*(5), 433-440.

805 Yeong, C. L. Y. & Torquato, S. (1998). Reconstructing random media. *Physical Review e,*
806 *57*(1), 495-506.

807 Zalc, J. M., Reyes, S. C., & Iglesia, E. (2004). The effects of diffusion mechanism and void
808 structure on transport rates and tortuosity factors in complex porous structures.
809 *Chemical Engineering Science, 59*(14), 2947-2960.

Table Captions

Table 1

Composition of the MF and UF concentrates.

Table 2

Values of parameters characterizing the microstructure of two concentrated milk suspensions (MF- and UF-suspensions) obtained from image analysis on binary micrographs[1].

Table 3

Values of parameters characterizing the microstructure of two concentrated milk gels (MF- and UF-gels) obtained from image analysis on binary micrographs[1].

Figure Captions

Fig. 1. Schematic representation of the automated segmentation procedure. The original TEM micrograph (A) is divided by a background image (B) to obtain a normalized image (C). The protein network is enhanced using a black top-hat filter (D), and smoothed to remove acquisition noise (E). Gray level histogram of the image, showing two peaks corresponding to the dark and white phases (F). The application of the Otsu threshold results in a binary image showing the protein phase as black and the void (aqueous) phase as white (G).

Fig. 2. Generation of a synthetic suspension of micelles. (A) 3D representation of a sample of the system of spheres (red) together with the region corresponding to the thick section (blue). (B) Sample binary image obtained by the intersection of the thick section with the system of spheres, projected along the z direction.

Fig. 3. Schematic representation of the microstructural parameters determined for dairy systems (suspensions and gels) by the image morphological granulometry method.

Fig. 4. Graphical illustration of tortuosity through a given point in a synthetic binary structure, computed as the ratio of the shortest lengths to borders (dashed line) over the image width (black line).

Fig. 5. TEM micrographs of concentrated milk suspensions and gels at 20000x magnification. (A) MF-suspension; (B) UF-suspension; (C) MF-gel; (D) UF-gel.

Fig. 6. Representative segmented TEM micrographs (binarised images) of concentrated milk suspensions and the related gels. (A) MF-suspension; (B) UF-suspension; (C) MF-gel; (D) UF-gel. These binarised images correspond to the TEM micrographs showed in Fig. 4.

Fig. 7. Distribution of particle sizes in TEM micrographs of (A) MF-suspension and (B) UF-suspension; Distribution of inter-particle distances in TEM micrographs of (C) MF-suspension and (D) UF-suspension.

Fig. 8. Distribution of particle aggregate sizes in TEM micrographs of (A) MF-gel and (B) UF-gel; Distribution of inter-particle aggregate distances in TEM micrographs of (C) MF-gel and (D) UF-gel.

Product	Dry matter (g/kg)	Caseins (g/kg)	Whey proteins (g/kg)	Lactose and Minerals (g/kg)	Other (g/kg)
MF concentrate	196	130.3	4.4	60.1	1.6
UF concentrate	223	130.7	27.3	63.1	1.8

Parameter	MF-suspension	UF-suspension
Area fraction	0.34 ± 0.02	0.33 ± 0.01
Porosity	0.66 ± 0.02	0.67 ± 0.01
Boundary length per unit area (μm/μm^2)	13.3 ± 0.5	12.1 ± 0.2*
Particle size (nm)	88 ± 3	99 ± 4*
Inter-particle distance (nm)	123 ± 5	132 ± 2*
Tortuosity	1.08 ± 0.01	1.06 ± 0.01

[1]The results are expressed as the mean ± standard deviation of the mean (n = 10).
* The means within a single row are significantly different ($p < 0.05$).

Parameter	MF-gel	UF-gel
Area fraction	0.49 ± 0.03	0.50 ± 0.02
Porosity	0.51 ± 0.03	0.50 ± 0.02
Boundary length per unit area (μm/μm^2)	9.5 ± 0.3	10.7 ± 0.7*
Particle aggregate size (nm)	141 ± 3	135 ± 8*
Inter-particle aggregate distance (nm)	147 ± 5	131 ± 7*
Tortuosity	1.5 ± 0.2	1.5 ± 0.2

[1]The results are expressed as the mean ± standard deviation of the mean (n = 10).
* The means within a single row are significantly different ($p < 0.05$).

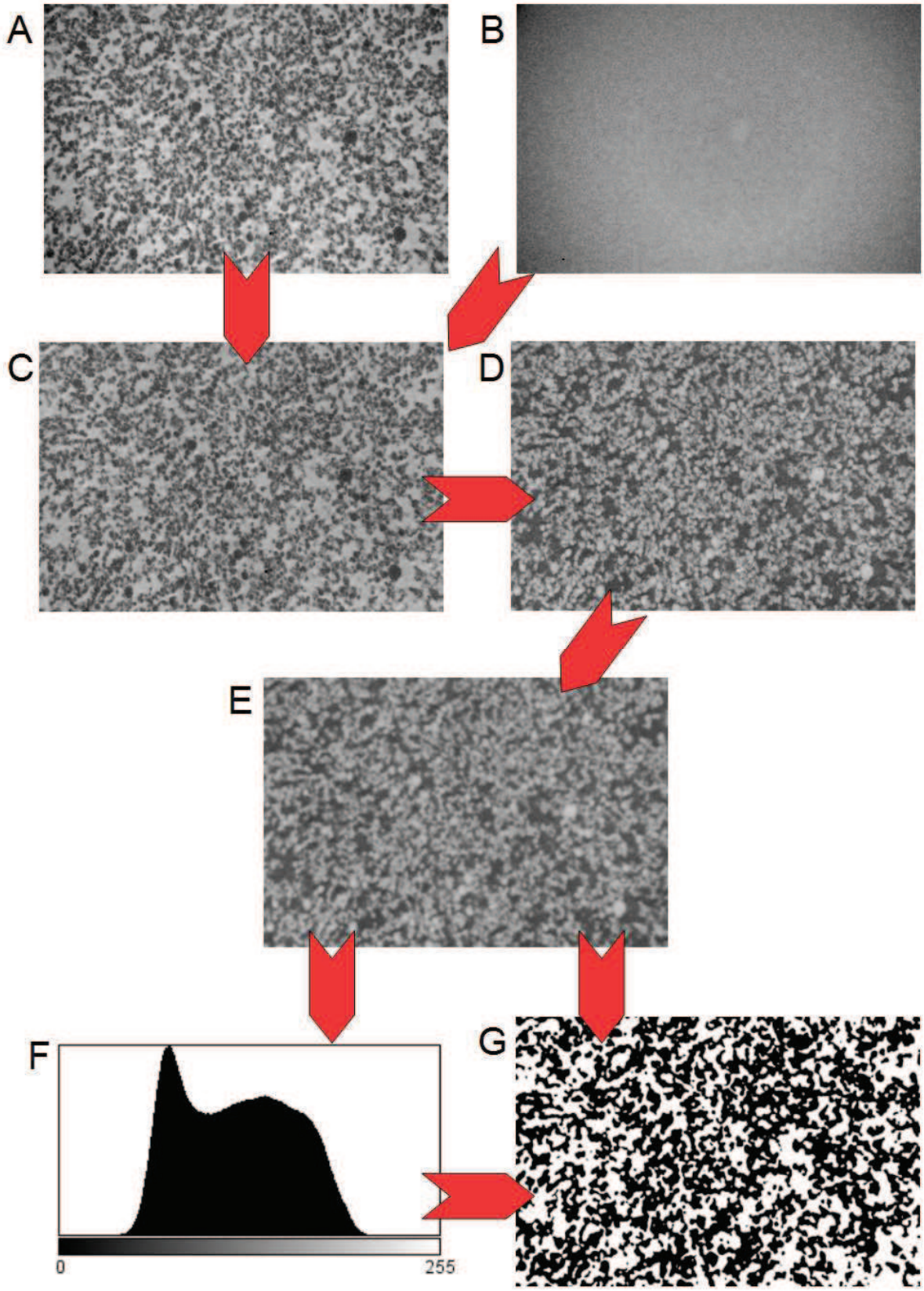
A
B
C
D
E
F
G
0
255

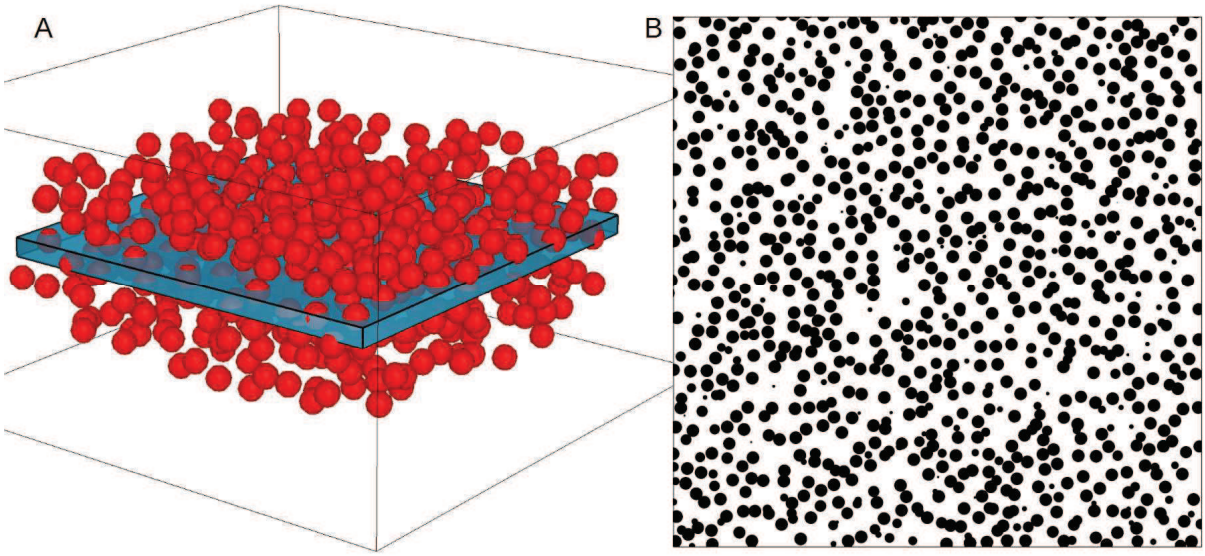

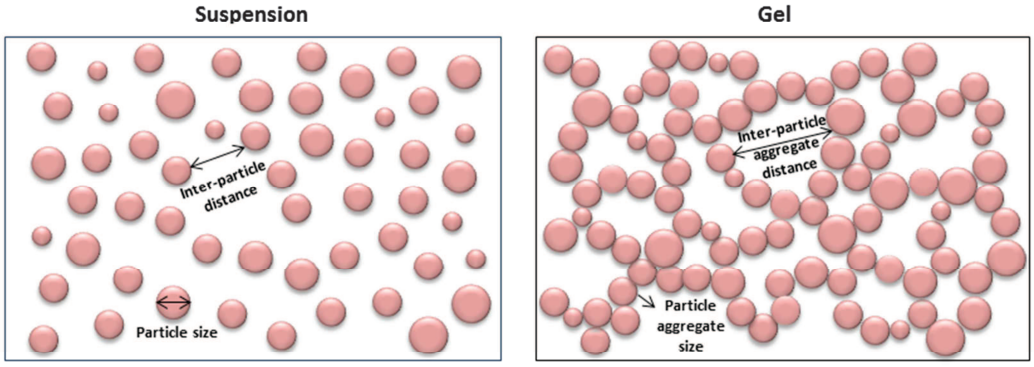

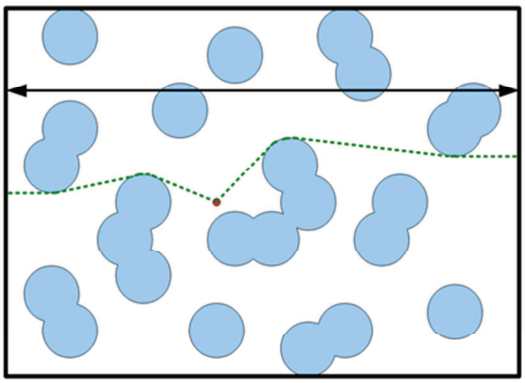

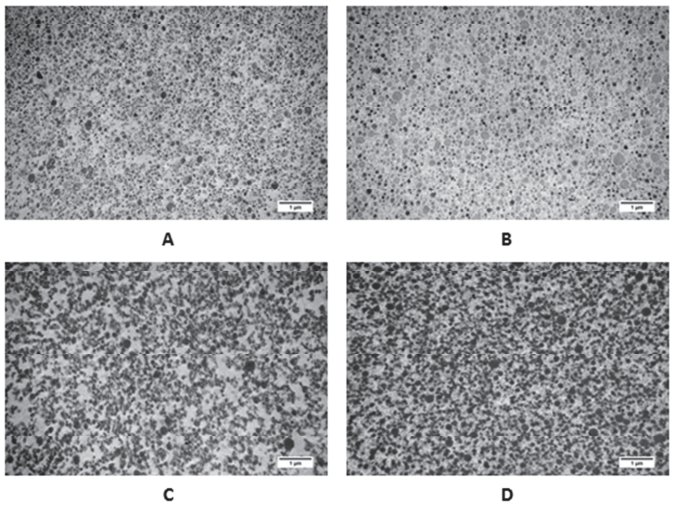

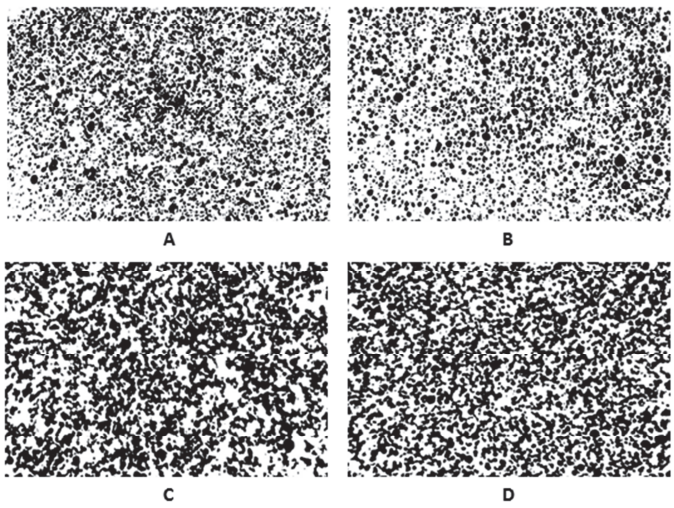

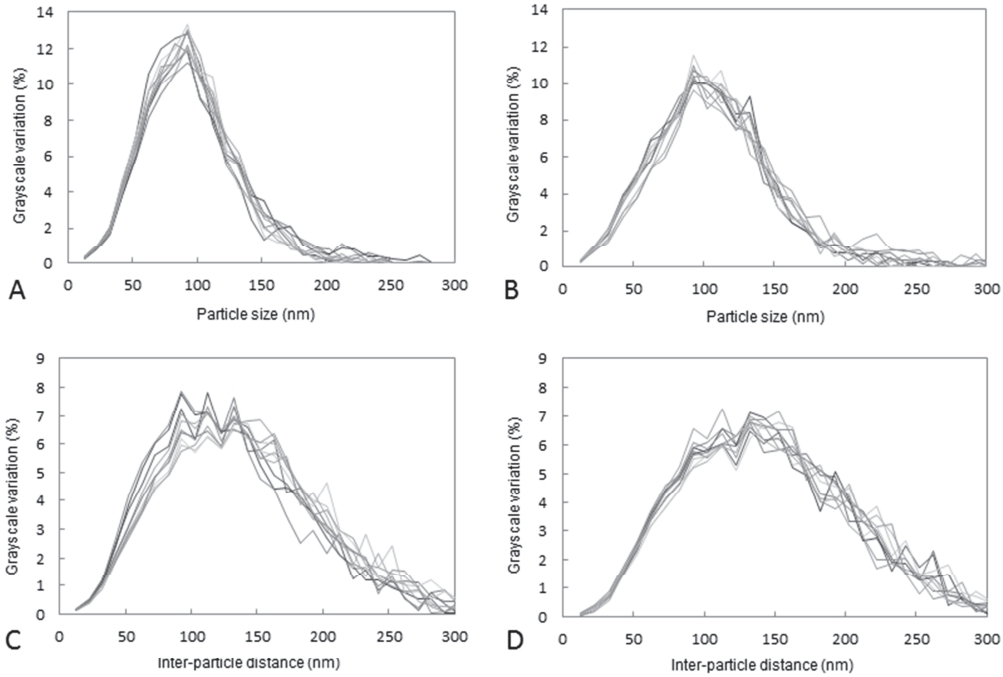

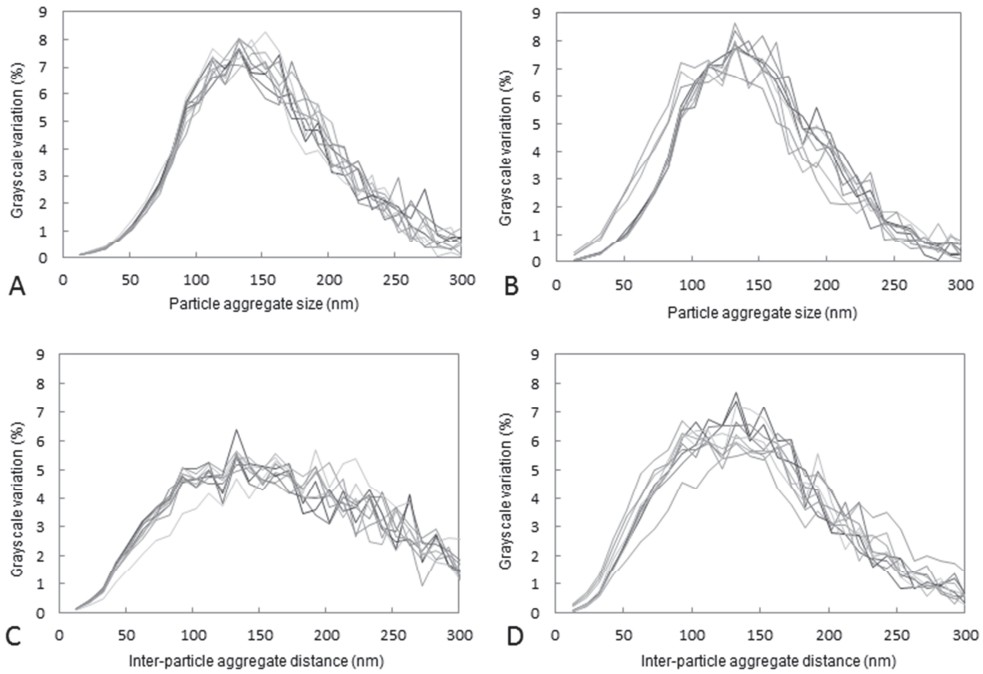

Highlights

- We developed a method of characterization of the microstructure of dairy systems.
- Microstructural parameters were determined by an automated image analysis method.
- These routine measurements provided discrimination between different dairy systems.
- This method applied to milk gels can be easily transferred to other food systems.